

# Analytical study of a nocturnal low-level jet over a shallow slope

A. SHAPIRO, E. FEDOROVICH

*School of Meteorology, University of Oklahoma, 120 David L. Boren Blvd., NORMAN (USA)*

## Abstract :

*A simple theory is presented for a nocturnal low-level jet (LLJ) over a planar slope. The theory extends the classical inviscid inertial-oscillation model of LLJs to include up- and downslope motion in the boundary layer within a stably-stratified environment. An initial value problem for the coupled equations of motion and thermodynamic energy is solved for air parcels suddenly freed of a frictional constraint near sunset. The notion of a tilted residual layer is introduced and used to relate initial (sunset) air parcel buoyancy to free-atmosphere stratification and thermal structure of the boundary layer.*

*Une théorie simple est présentée pour un courant-jet de basse couche, nocturne, le long d'un pan incliné. La théorie prolonge le modèle classique à oscillations d'inertie pour un fluide non visqueux en y incluant les mouvements ascendants et descendants au sein de la couche limite en milieu stratifié stable. Un problème aux valeurs initiales pour les équations couplées du mouvement et de l'énergie est résolu pour une parcelle d'air se trouvant soudainement libérée de toute contrainte visqueuse au coucher du soleil. Le concept de couche résiduelle inclinée est introduit et utilisé pour relier la flottabilité initiale de la parcelle à la stratification d'une atmosphère libre et à la structure thermique de la couche limite atmosphérique.*

**Key words :** low-level jet, inertial oscillation, planar slope, stable stratification, residual layer

## 1 Introduction

The nocturnal low-level jet (LLJ) – a sharp low-altitude maximum in the wind profile – is a warm-season boundary-layer phenomenon that commonly occurs over the Great Plains of the United States and many other places worldwide, typically in regions east of mountain ranges or in the vicinity of strong land–sea temperature contrasts ([2], [7-9]). The LLJ develops around sunset, under dry cloud-free conditions conducive to strong radiational cooling, reaches a peak intensity in the early morning hours, and then dissipates shortly after dawn, with the onset of daytime convective mixing. Other signature features of this phenomenon are an anticyclonic turning (veering) of the wind vector with time, and the development of a pronounced supergeostrophic southerly wind maximum (jet) typically at levels less than 1 km above ground level, and frequently at levels less than 500 m above ground level.

Several theories have been advanced for the origin of LLJs. Blackadar [1] and Buajitti and Blackadar [4] described the nocturnal jet as an inertial oscillation that develops in response to the rapid stabilization of the boundary layer that occurs near sunset under relatively dry, cloud-free conditions. A different class of theories was advanced to explain the longitudinal preference of the Great Plains LLJ, namely the high frequency of LLJ formation over the sloping terrain of the Great Plains (peak around 100° W) rather than over the flatter terrain further east. Holton [6] studied the response of the boundary layer over a sloping surface to a relatively slow and deep volumetric heating. Bonner and Paegle [3] considered a time-varying eddy viscosity and geostrophic wind, with the periodicity of the geostrophic wind ascribed to the diurnal temperature cycle over sloping terrain. Their results were in reasonable agreement with observations, but the amplitude of the oscillation was sensitive to the magnitude of the geostrophic wind, the choice of viscosity, and the phase difference between variations of the viscosity and the geostrophic wind.

In the present study, we explore the effects of terrain slope, thermal boundary layer structure, environmental stratification and synoptic-scale pressure gradient force on LLJ evolution within a simple theoretical framework. Specifically, we extend the inviscid, one-dimensional Blackadar [1] theory to include slope angle and a coupling between the equations of motion and thermodynamic energy. Although this approach

is admittedly idealized, it leads directly to interesting findings concerning the possible role of terrain-associated baroclinicity in the evolution of nocturnal low-level jets.

## 2 Theory of low-level jet

We consider a scenario typical of LLJs over the Great Plains of the United States, where geostrophic winds blow over terrain that slopes down toward the east.

Consider the development of a nocturnal low-level jet in the atmospheric boundary layer over a planar slope of infinite extent (no edge effects) having slope angle  $\alpha$ . Our analysis proceeds in slope-following Cartesian coordinates with the  $x$ -coordinate pointing east and down the slope, and the  $y$ -coordinate pointing across the slope toward the north. The jet is envisioned as an inertial-gravity oscillation induced in the boundary layer by the sudden release of a frictional constraint near sunset ( $t = 0$ ), as in the Blackadar [1] theory. We restrict attention to the special case where the synoptic-scale pressure gradient force points toward the west (minus  $x$  direction), and the associated geostrophic wind  $v_G$  is southerly ( $v_G > 0$ ), a restriction also considered in [6]. The velocity vectors are constrained to lie within planes tangent to the slope. The corresponding coupled inviscid/non-diffusive equations of motion and thermodynamic energy are

$$\frac{du}{dt} = -b \sin \alpha + f v - f v_G, \quad (1)$$

$$\frac{dv}{dt} = -f u, \quad (2)$$

$$\frac{db}{dt} = u N^2 \sin \alpha, \quad (3)$$

where  $u$  is the downslope velocity component,  $v$  is the cross-slope ( $v > 0$  is southerly) velocity component,  $b$  is buoyancy [ $b \equiv g(\theta - \theta_e) / \theta_r$ , where  $g$  is the gravitational acceleration,  $\theta$  is the potential temperature,  $\theta_e$  is a height-varying environmental potential temperature, that is, the potential temperature in the free atmosphere, and  $\theta_r$  is a constant reference potential temperature],  $N \equiv \sqrt{(g / \theta_r) d\theta_e / dz}$  is the free-atmosphere Brunt-Väisälä frequency, and  $f$  is the Coriolis parameter. The latter three parameters are considered constant and positive, so the geostrophic wind is constant and southerly, the free-atmosphere stratification is constant and stable, and the flow takes place in the Northern hemisphere. It should also be born in mind that since  $-f v_G$  is a proxy for the pressure gradient force, the pressure gradient force is treated as constant. In arriving at the Coriolis terms in this coordinate system, we replaced the exact form of the slope-normal component of the Earth's angular velocity by the true vertical component. This rather mild approximation is commonly used in idealized one-dimensional models of katabatic flows with provision for the Coriolis force.

One must impose in (1)-(3) the initial values of  $u$ ,  $v$  and  $b$ , that is, the values upon the release of the frictional constraint near sunset. Far above the boundary layer, the solution corresponding to  $v = v_G$  (initially) is simply  $v(t) = v_G$ ,  $u(t) = 0$ , and  $b(t) = 0$ , that is, the flow is geostrophic at all times. Within the boundary layer, the effects of afternoon heating can be taken into account by specifying the buoyancy as an initial (sunset) condition. A positive value of buoyancy at a location within the sloping boundary layer implies that a positive potential temperature difference exists between the air at that location and the environmental air at the same elevation.

Eliminating in (1)-(3)  $v$  and  $b$  in favor of  $u$  yields

$$\frac{d^2 u}{dt^2} = -\omega^2 u, \quad (4)$$

where

$$\omega \equiv \sqrt{f^2 + N^2 \sin^2 \alpha} = f \sqrt{1 + \text{Bu}} \quad (5)$$

and  $\text{Bu} \equiv N^2 \sin^2 \alpha / f^2$  is the slope Burger number. The general solution of (4) is

$$u = A \cos \omega t + D \sin \omega t. \quad (6)$$

Applying (6) in (2) and integrating the result yields  $v$  as

$$v = -\frac{f}{\omega} (A \sin \omega t - D \cos \omega t) + C. \quad (7)$$

We then obtain  $b$  as a residual from (1):

$$b = \frac{N^2 \sin \alpha}{\omega} (A \sin \omega t - D \cos \omega t) + \frac{f}{\sin \alpha} (C - v_G). \quad (8)$$

Application of the initial conditions  $b(0) = b_0$ ,  $u(0) = u_0$ ,  $v(0) = v_0$  in (6)-(8), yields  $A$ ,  $D$ ,  $C$  as

$$A = u_0, \quad D = \frac{1}{\omega} [-b_0 \sin \alpha + f(v_0 - v_G)], \quad C = \frac{N^2 \sin^2 \alpha}{\omega^2} v_0 + \frac{f}{\omega^2} (b_0 \sin \alpha + f v_G). \quad (9)$$

After introducing the non-dimensional variables

$$\begin{aligned} U &\equiv \frac{u}{v_G}, & V &\equiv \frac{v}{v_G}, & B &\equiv \frac{b \sin \alpha}{f v_G}, & T &\equiv f t, & \Omega &\equiv \frac{\omega}{f} = \sqrt{1 + \text{Bu}}, \\ U_0 &\equiv \frac{u_0}{v_G}, & V_0 &\equiv \frac{v_0}{v_G}, & B_0 &\equiv \frac{b_0 \sin \alpha}{f v_G}, \end{aligned} \quad (10)$$

the solution for the flow variables expressed as deviations from initial values becomes

$$U(T) - U_0 = U_0 (\cos \Omega T - 1) + \frac{1}{\Omega} (-B_0 + V_0 - 1) \sin \Omega T, \quad (11)$$

$$V(T) - V_0 = -\frac{U_0}{\Omega} \sin \Omega T + \frac{1}{\Omega^2} (-B_0 + V_0 - 1) (\cos \Omega T - 1), \quad (12)$$

$$B(T) - B_0 = \frac{\Omega^2 - 1}{\Omega} U_0 \sin \Omega T - \frac{\Omega^2 - 1}{\Omega^2} (-B_0 + V_0 - 1) (\cos \Omega T - 1). \quad (13)$$

The cross-isobar wind component is typically much smaller than the geostrophic wind speed. Accordingly, we take  $U_0 = 0$ . For simplicity we also take  $B_0 = 0$ , although we also later consider a non-zero  $B_0$  flow case. Time series of  $U(T)$ ,  $V(T)$  and  $B(T)$  are shown in Fig. 1 for two subgeostrophic values of the southerly wind component,  $V_0 = 0.4$  and  $V_0 = 0.8$ . Results are presented for latitude  $35^\circ\text{N}$  ( $f = 8.3 \times 10^{-5} \text{s}^{-1}$ ) with  $N = 0.01 \text{s}^{-1}$ , and five slope angles:  $0^\circ$  ( $\text{Bu}=0$ ),  $0.15^\circ$  ( $\text{Bu}=0.1$ ),  $0.5^\circ$  ( $\text{Bu} = 1.1$ ), and  $1^\circ$  ( $\text{Bu} = 4.4$ ). The  $\text{Bu} = 0$  case corresponds to the original Blackadar [1] scenario, while the  $0.15^\circ$  angle characterizes the slope of the Texas and Oklahoma panhandles (around  $100^\circ \text{W}$ ) and is close to the  $1/400$  slope considered in [6]. The  $0.5^\circ$  angle is an upper bound for the slope of the High Plains of eastern Colorado and New Mexico.

### 3 Results

The flow behavior depicted in Fig. 1 is readily explained by considering (1)-(3). Shortly after the release of the frictional constraint, the now-unopposed westward-pointing pressure gradient force ( $-f v_G$ ) induces an up-slope wind ( $u < 0$ ). Associated with this up-slope wind is a Coriolis force ( $-f u$ ) which induces an increase in the southerly wind component. However, the up-slope wind also advects environmental potential temperature up the slope, which decreases the buoyancy ( $b < 0$ ) and produces a positive downslope buoyancy force ( $-b \sin \alpha$ ). The increasing value of the Coriolis force  $f v$  and the increasing value of the downslope buoyancy force both oppose the pressure gradient force, and lead to a decrease in the magnitude of  $u$ , and eventually to a reversal in the sign of  $u$ . Figure 1 also shows that zeroes in  $u$  are associated with extrema in  $b$  and  $v$ , with maxima in  $v$  corresponding to minima in  $b$ . It can be shown that elimination of  $b$  in (1)-(3) followed by an integration yields an equation for a velocity hodograph in a form of an ellipse.

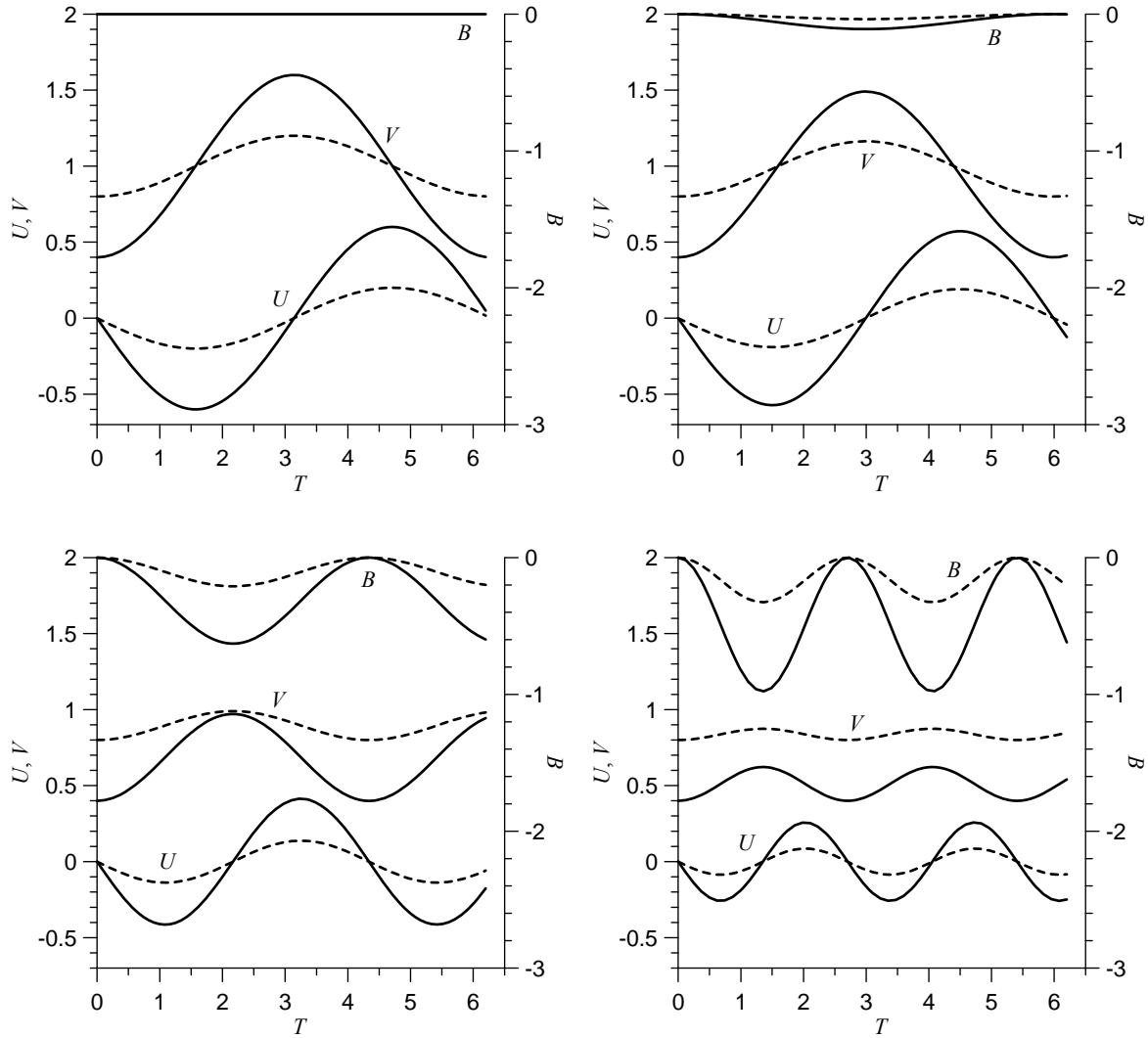


FIG. 1 – Time series of  $U$ ,  $V$ ,  $B$  at latitude  $35^\circ\text{N}$  with Brunt-Väisälä frequency  $N = 0.01\text{s}^{-1}$  for four slope angles:  $0^\circ$  ( $Bu=0$ ; upper left),  $0.15^\circ$  ( $Bu=0.1$ , upper right),  $0.5^\circ$  ( $Bu = 1.1$ , lower left), and  $1^\circ$  ( $Bu = 4.4$ , lower right). Results are presented for two initial values of the southerly wind component,  $V_0 = 0.4$  (solid lines) and  $V_0 = 0.8$  (dashed lines).

Initial values of  $U$  and  $B$  are 0. Note that the  $B$  axes are on the right side of each figure ( $B$  is negative). All plotted variables are nondimensional.

After the time of sunset, the layer formerly mixed by dry-convective thermals is replaced by a so-called residual layer, whose thermal structure is largely unchanged from its well-mixed late-afternoon state, and whose potential temperature is nearly independent of height. The residual layer extends upward to a relatively thin capping inversion at the base of the free atmosphere. If we apply the notion of residual layer to the atmosphere over a slightly-inclined slope and keep in mind that parcel buoyancy is proportional to the potential temperature difference between the parcel and the environment at the same elevation, then we are led to the concept of a tilted residual layer (TRL) illustrated in Fig. 2. Taking potential temperature  $\theta$  approximately constant ( $= \theta_0$ ) from point J (corresponding to the initial/sunset location of an air parcel) up to the base of the capping inversion (where it increases by  $\Delta\theta$ ), provides  $\theta = \theta_0 + \Delta\theta$  at point K. The horizontal line from K to a point L is an environmental isentrope, and so the potential temperature at L is also  $\theta_0 + \Delta\theta$ . Since the potential temperature decreases from point L to point M (where M is in the free atmosphere location beneath point L, at the same elevation as the parcel at J) by  $\delta d\theta_e/dz$ , where  $\delta (> 0)$  is the altitude difference between points L and M, the potential temperature at M is  $\theta_0 + \Delta\theta - \delta d\theta_e/dz$ .

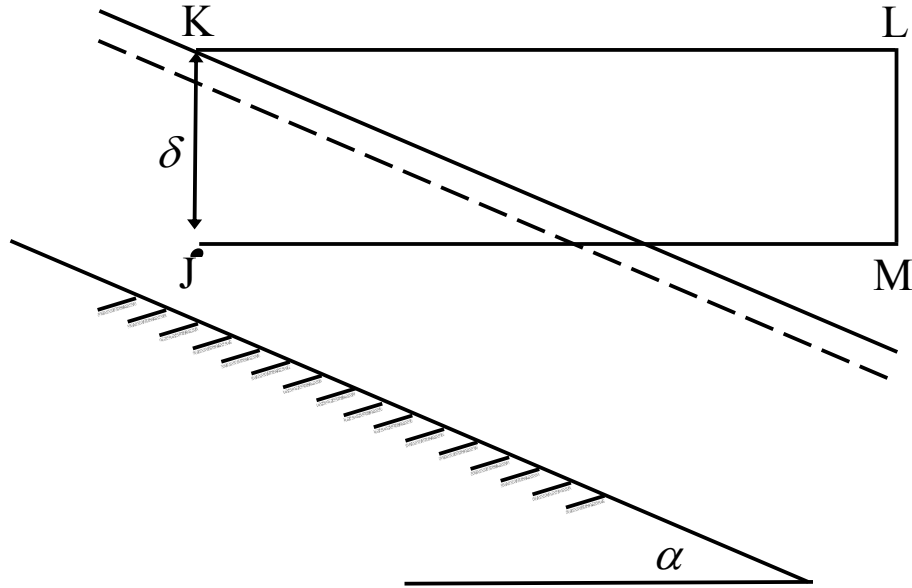


FIG. 2 – Vertical cross-section through a residual layer over a shallow slope. Dashed line marks the base of the inversion layer. Sloping solid line passing through point K marks the top of the inversion layer. Symbol J marks the position of an air parcel within the residual layer,  $\delta$  is the distance of the parcel from the top of the capping inversion, point L is in the free atmosphere at the same elevation as point K, point M is in the free atmosphere directly beneath L, at the same elevation as J. The horizontal line KL indicates an environmental isentrope.

Thus, the initial buoyancy for the parcel at J is  $b_0 = -g\Delta\theta/\theta_r + N^2\delta$ , and the corresponding non-dimensional buoyancy is

$$B_0 = \frac{N^2 \sin \alpha}{f v_G} \delta - \frac{\sin \alpha}{f v_G} \frac{g\Delta\theta}{\theta_r}. \quad (14)$$

Since  $\delta$  decreases with increasing slope-normal coordinate, the slope-normal derivative of  $B_0$  (and of  $b_0$ ) is negative (buoyancy decreases upward) and has a magnitude proportional to  $N^2$ , that is, it is very strongly dependent on the free-atmosphere static stability.

Applying (14) in (12) at the time  $T = \pi/\Omega$  when  $V$  attains a peak amplitude  $V_{\max}$  (again taking  $U_0 = 0$ ) yields

$$V_{\max} = V_0 \left( 1 - \frac{2f^2}{f^2 + N^2 \sin^2 \alpha} \right) + \frac{2f^2}{f^2 + N^2 \sin^2 \alpha} \left( \frac{N^2 \sin \alpha}{f v_G} \delta - \frac{\sin \alpha}{f v_G} \frac{g\Delta\theta}{\theta_r} + 1 \right). \quad (15)$$

From (15) we infer that the large values of  $V_{\max}$  are obtained for parcels with small values of  $V_0$  (large initial ageostrophic wind speed  $1 - V_0$ ) located at low levels (large  $\delta$ ) within a residual layer with a weak capping inversion (small  $\Delta\theta$ ). Predicted values of  $V_{\max}$  are shown in Fig. 3 for a relatively strong initial wind ( $V_0 = 0.8$ ) typical of a boundary layer that has undergone vigorous daytime convective mixing. In most of the plotted curves, as  $\alpha$  increases from  $0^\circ$ ,  $V_{\max}$  increases at first, and then decreases. The increase and subsequent decrease are particularly striking in the case of stronger stratification with peak jet winds exceeding the geostrophic winds by a factor of two. Evidently, for small  $\alpha$ , the tendency of a positive initial buoyancy to strengthen the amplitude of the oscillation overcomes the inhibiting influence of advection of environmental potential temperature, but for the larger slope angles, advection of environmental potential temperature dominates. The free-atmosphere stratification plays two contrasting roles in our theory. On one hand, it directly inhibits the amplitude of the inertial-gravity oscillation by cooling parcels ascending the slope and warming parcels descending the slope (via advection of environmental potential temperature). On the other hand, it is also associated (within the TRL conceptual framework) with positive initial values of buoyancy, which result in more vigorous inertial-gravity oscillations.

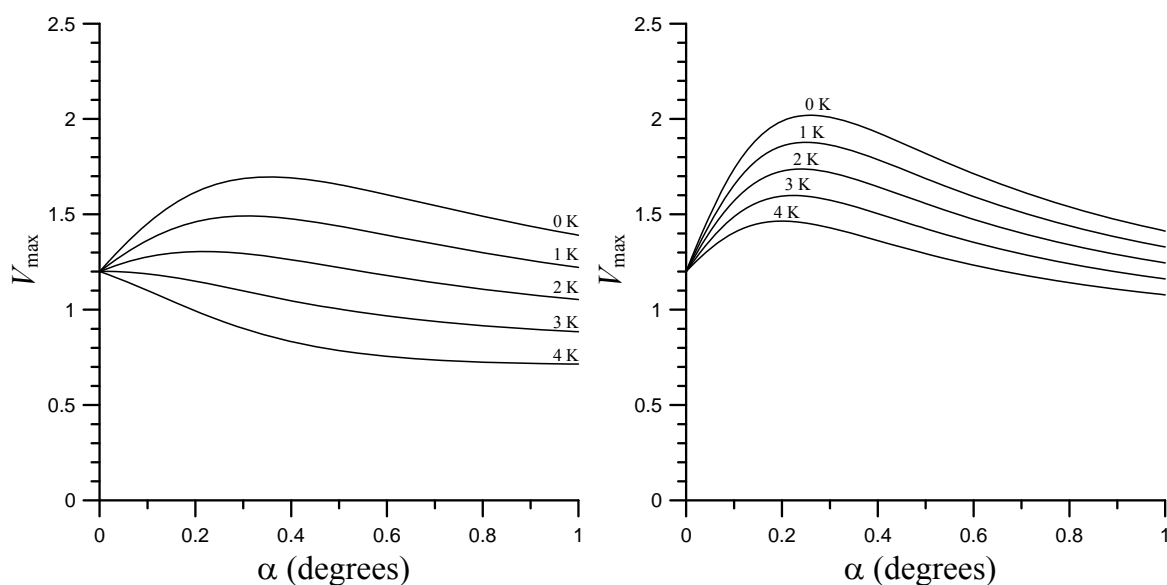


FIG. 3 – Peak southerly jet speed  $V_{\max}$  as a function of slope angle  $\alpha$  for a parcel with initial southerly wind component  $V_0 = 0.8$  located 1000 m beneath a capping inversion. Results are shown for five capping inversion strengths,  $\Delta\theta = 0, 1, 2, 3, 4$  K, and two values of  $N$ ,  $0.01\text{s}^{-1}$  (left panel), and  $0.015\text{s}^{-1}$  (right panel).

#### 4 Summary

Our theory yields the following predictions for the structure and behavior of the Great Plains low level jet:

- When drawn on the hodograph plain, the jet evolves as an ellipse with major axis aligned with the  $u$ -wind component. This result is consistent with observations.
- Following the proposed TRL model, the strongly supergeostrophic winds observed in some real jets are accounted for in our theory by including sloping terrain and initial parcel buoyancies.
- The initial (sunset) buoyancy profile within the TRL provides conditions for the flow over the slope to develop a jet-like velocity profile from a well-mixed (uniform) initial velocity field.
- The theory predicts the existence of an optimum slope angle associated with peak jet strength.

#### References

- [1] Blackadar, A. K., *Boundary layer wind maxima and their significance for the growth of nocturnal inversions*, *Bull. Amer. Meteor. Soc.*, **38**, 283-290, 1957.
- [2] Bonner, W. D., *Climatology of the low level jet*, *Mon. Wea. Rev.*, **96**, 833-850, 1968.
- [3] Bonner, W. D., and J. Paegle, *Diurnal variations in boundary layer winds over the south-central United States in summer*, *Mon. Wea. Rev.*, **98**, 735-744, 1970.
- [4] Buajitti, K., and A. K. Blackadar, *Theoretical studies of diurnal wind-structure variations in the planetary boundary layer*, *Quart. J. Roy. Meteor. Soc.*, **83**, 486-500, 1957.
- [6] Holton, J. R., *The diurnal boundary layer wind oscillation above sloping terrain*, *Tellus*, **19**, 199-205, 1967.
- [7] Stensrud, D. J., *Importance of low-level jets to climate: A review*, *J. Climate*, **9**, 1698-1711, 1996.
- [8] Walters, C. K., J. A. Winkler, R. P. Shadbolt, J. van Ravensway, and G. D. Bierly, *A long-term climatology of southerly and northerly low-level jets for the central United States*, *Annals Assoc. Amer. Geog.*, **98**, 521-552, 2008.
- [9] Whiteman, C. D., X. Bian, and S. Zhong, *Low-level jet climatology from enhanced rawinsonde observations at a site in the southern Great Plains*, *J. Appl. Meteor.*, **36**, 1363-1376, 1997.